Chronic GLP-1 Receptor Activation by Exendin-4 Induces Expansion of Pancreatic Duct Glands in Rats and Accelerates Formation of Dysplastic Lesions and Chronic Pancreatitis in the Kras^{G12D} Mouse Model

Belinda Gier,[1] Aleksey V. Matveyenko,[1] David Kirakossian,[1] David Dawson,[2,3] Sarah M. Dry,[2,3] and Peter C. Butler[1,3]

Pancreatic duct glands (PDGs) have been hypothesized to give rise to pancreatic intraepithelial neoplasia (PanIN). Treatment with the glucagon-like peptide (GLP)-1 analog, exendin-4, for 12 weeks induced the expansion of PDGs with mucinous metaplasia and columnar cell atypia resembling low-grade PanIN in rats. In the pancreata of Pdx1-Cre; LSL-Kras^{G12D} mice, exendin-4 led to acceleration of the disruption of exocrine architecture and chronic pancreatitis with mucinous metaplasia and increased formation of murine PanIN lesions. PDGs and PanIN lesions in rodent and human pancreata express the GLP-1 receptor. Exendin-4 induced proproliferative signaling pathways in human pancreatic duct cells, cAMP–protein kinase A and mitogen-activated protein kinase phosphorylation of cAMP-responsive element-binding protein, and increased cyclin D1 expression. These GLP-1 effects were more pronounced in the presence of an activating mutation of Kras and were inhibited by metformin. These data reveal that GLP-1 mimetic therapy may induce focal proliferation in the exocrine pancreas and, in the context of exocrine dysplasia, may accelerate formation of neoplastic PanIN lesions and exacerbate chronic pancreatitis. ***Diabetes*** **61:1250–1262, 2012**

Glucagon-like peptide (GLP)-1 is a proglucagon-derived peptide secreted by gut endocrine cells (L cells) in response to meal ingestion (1). The GLP-1 receptor (GLP-1R) is a G-protein–coupled receptor that is expressed in pancreatic islets and exocrine duct cells (2,3). The increased GLP-1 released after meal ingestion amplifies postprandial nutrient-driven insulin secretion, the so-called incretin effect (4). Based on this property, GLP-1R activation became an attractive therapeutic target for type 2 diabetes mellitus (T2DM).

To overcome the short half-life of circulating GLP-1 that is rapidly degraded by dipeptidyl peptidase (DPP)-4 (5), two strategies have been used in drug development. Oral DPP-4 small molecule inhibitors, such as sitagliptin, prolong the half-life of endogenously secreted GLP-1 (6). Alternatively, GLP-1R peptide agonists given by injection, such as exenatide (7) and liraglutide (8), are resistant to DPP-4 degradation.

Pancreatitis emerged as an unexpected side effect of GLP-1–based therapy in case reports (9,10), and in the U.S. Food and Drug Administration adverse-event reports, liraglutide and sitagliptin showed a signal of pancreatitis (11–13), although analysis of insurance claims records have been reported to show no association between GLP-1–based therapy and pancreatitis (14). Because the human pancreas is inaccessible in treated patients, the question as to whether GLP-1 mimetic therapy acts on the exocrine pancreas has been a subject of animal-based studies.

Pancreatic duct cell proliferation increased transiently with a GLP-1 infusion in Wistar rats (15). Sprague-Dawley rats treated with exendin-4 for 12 weeks developed low-grade chronic pancreatitis (16). Furthermore, DPP-4 inhibition with sitagliptin for 12 weeks was associated with increased pancreatic duct cell replication and acinar-to-ductal metaplasia and, in 1 of 10 rats, chronic pancreatitis (3). However, GLP-1–based therapy also has been reported to not exacerbate chemically induced pancreatitis in mice (17). Also, exenatide was reported to have no effect on ductal turnover in mice or rats, as well as to have a beneficial action in chemically induced pancreatitis (18).

Pancreatic duct glands (PDGs), under conditions of chronic injury, such as chemically induced pancreatitis, may give rise to lesions resembling pancreatic intraepithelial neoplasia (PanIN) (19). To date, there is no information on the actions of GLP-1–based therapy on PDGs or the development of PanIN in pancreata predisposed to dysplasia. Here, we sought to address the following questions. First, does chronic activation of GLP-1Rs by exendin-4 lead to proliferation of the PDGs? Second, is GLP-1R expression present in PDGs and PanIN-like dysplastic lesions? Third, does chronic activation of GLP-1Rs alter the phenotype of Pdx1-Cre; LSL-Kras^{G12D} (Pdx1-Kras) mice?

RESEARCH DESIGN AND METHODS

Rodent studies. All animal studies were approved by the animal use and care committee at the University of California Los Angeles (UCLA). Animals were housed individually in a 12-h light/dark cycle and were weighed weekly to adjust drug doses. Blood glucose and food intake were monitored on a biweekly basis.

Sprague-Dawley rats treated with exendin-4. To establish the actions of GLP-1R activation in the exocrine pancreas, we treated 10 male Sprague-Dawley rats (Charles River Laboratories, Wilmington, MA) with daily injections of 10 μg/kg body wt exendin-4 (ChemPep, Miami, FL) administered by subcutaneous injection for 12 weeks starting at 10 weeks of age (20). Animals were fed chow (Teklad; Harlan Laboratories, Madison, WI) ad libitum. A total

From the [1]Larry L. Hillblom Islet Research Center, University of California Los Angeles (UCLA), David Geffen School of Medicine, Los Angeles, California; the [2]Department of Pathology and Laboratory Medicine, UCLA, David Geffen School of Medicine, Los Angeles, California; and the [3]Jonsson Comprehensive Cancer Center, UCLA, David Geffen School of Medicine, Los Angeles, California.

Corresponding author: Belinda Gier, bgier@mednet.ucla.edu.

Received 8 August 2011 and accepted 16 November 2011.

DOI: 10.2337/db11-1109

This article contains Supplementary Data online at http://diabetes.diabetesjournals.org/lookup/suppl/doi:10.2337/db11-1109/-/DC1.

See accompanying articles, pp. 986, 989, and 1243.

of 15 control rats received daily saline injections. We did not identify PDGs in 5 of 15 controls; therefore, these 5 rats were not included in subsequent analyses. PDGs were identified in all treated rats.

Pdx1-Kras mice treated with exendin-4. To investigate the effect of chronic GLP-1 mimetic treatment on pancreatic cancer precursor lesions, the conditional $Kras^{G12D}$ from Hingorani et al. (21) was used. Experimental animals were generated by crossing Pdx1-Cre with LSL-$Kras^{G12D}$ mice on a C57/BL6 background (both gifts of Guido Eibl, UCLA). Mice (6 weeks old) were fed an AIN-76A–based diet (Research Diets, New Brunswick, NJ) ad libitum for 12 weeks, during which either saline (n = 7) or exendin-4 (5 nmol/kg body wt) (n = 5) was injected subcutaneously daily.

Pancreas fixation, embedding, and sectioning

Rat pancreas. After the rats were killed, the rat pancreata were rapidly dissected and then divided into two portions (the head and body of the pancreas and the tail of the pancreas). These were fixed in 4% paraformaldehyde overnight at 4°C and embedded in paraffin, oriented flat to permit subsequent microscopic sections to be made through the longitudinal plane of the pancreas. The block containing the head and body of the pancreas was sectioned at 4-μm intervals to obtain a minimum of 40 sections through the longitudinal plane of the pancreas. A minimum of 10 serial sections were obtained per block from the tail of the pancreas.

Mouse pancreas. Successful excision-recombination events were confirmed by genotyping analysis (Transnetyx, Cordova, TN). Paraformaldehyde-fixed, paraffin-embedded pancreatic sections (4 μm) of whole pancreas were stained as below.

Human pancreas. Paraffin-embedded tissue blocks of nonneoplastic human pancreata adjacent to surgically resected pancreatic adenocarcinoma were selected from 10 case subjects from the UCLA pathology archives. All slides and tissue blocks were retrieved after institutional review board approval (no. 11-001724).

Pancreas histology and stains. Tissue sections from rats and mice were deparaffinized in toluene and rehydrated in an ethanol gradient. First, sections were stained in Harris hematoxylin solution (HHS16; Sigma) and eosin Y solution (HT110132; Sigma) to evaluate general histology. PDGs were defined based on the previously described criteria (19) (Fig. 1). Sections were stained by Alcian blue (Electron Microscopy Sciences) and *p*-aminosalicylic acid (PAS) (Sigma).

For immunhistochemical-immunofluorescent staining, antigen retrieval was performed via microwave heating in citrate buffer (H-3300; Vector, Burlingame, CA), and slides were blocked in Tris-buffered saline (3% bovine serum albumin, 0.2% TX-100, and 2% bovine serum) for 1 h. The following primary antibodies were used for the 12-h incubation (4°C): ductal cell marker cytokeratin (mouse anti-pancytokeratin, 1:50 [Sigma] or rat anti-cytokeratin19/TROMAIII, 1:100 [Hybridoma Bank, University of Iowa, Iowa City, IA]); acinar cell marker amylase (rabbit anti-amylase, 1:300; Abcam); proliferation marker anti–Ki-67 (1:50; Dako, Carpinteria, CA); GLP-1R (rabbit anti-human GLP-1R, NLS1206, 1:100; Novus Biologicals, Littleton, CO); and pancreatic and duodenal homeobox-1 (Pdx-1) (rabbit anti–Pdx-1, 1:500; β-Cell Biology Consortium, Nashville, TN). Validation of the GLP-1R antisera, NLS1206, was published previously (22). Secondary antibodies labeled with Cy3 and fluorescein isothiocyanate were obtained from The Jackson Laboratories (West Grove, PA) and used at dilutions of 1:100 for the 1-h incubation at room temperature.

For immunohistochemical staining, endogenous peroxidase activity was quenched with 10% methanol, 10% H_20_2 in Tris-buffered saline, followed by incubation with anti–Ki-67 (dilution 1:100; Dako) for 12 h (4°C). Subsequent detection was performed with Envision+ anti-rabbit horseradish peroxidase (Dako), with 3′,3′-diaminobenzidine used as the chromogen and hematoxylin as the counterstain.

Likewise, sections of human pancreata were stained with hematoxylin and eosin, Alcian blue, and PAS in order to permit the identification of PDGs and PanIN lesions. Sections adjacent to those with PDGs and PanIN lesions also were stained by immunofluorescence for cytokeratin and for GLP-1R (the same antibodies and dilution as above).

Morphometric analysis of the pancreatic duct gland compartment in rats. The slide with the greatest number of PDGs per animal was selected for quantitative analysis. Slides were digitally scanned in the UCLA Translational Pathology Core Laboratory using an Aperio ScanScope XT (Aperio Technologies, Vista, CA). Quantitative analysis was performed using Aperio Scanscope software. The length of the large duct associated with PDGs and the mean cross-sectional area per PDG were measured in each case. PDGs in the exendin-4–treated rats often showed complex epithelial architecture, including cribiform patterns and pseudopapillae, consistent with epithelial proliferation. The ducts containing this complex PDG epithelial architecture appeared more dilated. To quantify if ductal dilation was present, we measured the longest axis of the large ducts present (duct length) and the inner circumference of the duct lumen. This allowed us to compute a ratio (inner duct luminal circumference to duct length) for each animal.

Histological analysis of chronic pancreatitis and murine PanIN (mPanIN) lesions in Pdx1-Kras mice. Full histologic cross-sections of each pancreas were stained with hematoxylin and eosin for histopathologic examination by two subspecialty gastrointestinal pathologists (D.D. and S.M.D.) blinded to treatment conditions. Chronic pancreatitis was graded using a semiquantitative scoring system, as previously described (23), with slight modification. Chronic pancreatitis was given an index score (0–12) reflecting the sum of scores for acinar loss, lobular inflammation, and fibrosis. Acinar loss was based on the percentage loss across the entire cross-section and graded as 0, absent; 1, 1–25%; 2, 26–50%; 3, 51–75%; and 4, >75%. Inflammation was based on the average number of lobular inflammatory cells per 40× high power field (HPF) (as counted in 10 nonoverlapping HPFs) and graded as 0, absent; 1, 1–30 cells; 2, 31–50 cells; 3, 51–100 cells; and 4, >100 cells. Fibrosis was based on the cumulative area of stromal fibrosis across the entire pancreas and graded as 0, absent; 1, 1–5%; 2, 6–10%; 3, 11–20%; and 4, >20% fibrosis. Duct profiles were evaluated according to established consensus guidelines for the histologic evaluation of mPanIN (24) and quantified as previously described (25). All duct profiles in one full pancreas cross-section were evaluated to determine the relative proportions of nondysplastic (normal, reactive, and metaplastic) ducts and each category of mPanIN lesion. The proportion of each mPanIN lesion to the overall number of duct profiles was recorded for each animal.

Duct cell replication frequency. To determine the frequency of replication of PDG cells and cells in the adjacent main ducts in the head of the pancreas in rats, we quantified the percentage of Ki-67–positive cells. Thus, the total number of duct cells (the head of the pancreas) evaluated was 57,261 in exendin-4–treated rats and 61,298 in controls. We also evaluated the frequency of duct cell replication in the sections of the tail of the pancreas immunostained for cytokeratin and Ki-67. The total number of duct cells evaluated from the tail was 24,483 in exendin-4–treated rats and 19,796 in controls.

Duct cell replication in pancreata from Pdx1-Kras mice also was analyzed by Ki-67. The extensive acinar-to-ductal metaplasia and frequent dysplastic ductal lesions in GLP-1–treated Pdx1-Kras mice precluded distinguishing replication frequency in the various component of the ductal compartment (PDGs and normal and dysplastic ducts). Slides were analyzed using the Ariol SL-50 automated slide scanner (Leica Microsystems) to quantitate the amount of positive staining for each area of interest containing only ducts and dysplastic ductal tissue. A total number of 121,883 (control group) and 101,830 (exendin-4–treated group) cells were analyzed.

GLP-1 actions on pancreatic duct cells. In vitro experiments were carried out to investigate the effects of exendin-4 on human pancreatic duct epithelial (HPDE) cells (26,27). HPDE cells (kindly made available by Dr. Ming-Sound Tsao, University of Toronto) were maintained in keratinocyte serum-free media supplemented with bovine pituitary extract and human epidermal growth factor (Invitrogen) at 37°C with 5% CO_2. HPDE cells transfected with the empty vector (pBabepuro) (HPDE-pBP) or with oncogenic pBP-$Kras4B^{G12V}$ (HPDE-Kras) also were used to permit the assessment of GLP-1R activation in the presence of an activating Kras mutation.

To assess the effect of exendin-4 (10 nmol/L) on the phosphorylation of cAMP-responsive element-binding (CREB) protein and the mitogen-activated protein kinases (MAPKs) extracellular signal–related kinase (ERK) 1/2, as well as levels of the cyclin A and D1, 90,000 cells were seeded in six-well plates containing complete medium. At ~70% confluence (day 3 after plating), cells were rinsed with PBS and incubated in starvation medium (lacking bovine pituitary extract and human epidermal growth factor) for 24 h. HPDE cells containing either a control plasmid (pBabepuro; HPDE-pBP) or the mutated oncogenic pBP-$Kras^{G12V}$ (28,29) were pretreated with 100 μmol/L metformin for 30 min. For stimulation experiments, exendin-4 was added in fresh, prewarmed starvation medium for the indicated time points. Stimulation then was stopped by adding ice-cold PBS, and HPDE cells were lysed in lysis buffer (50 mmol/L Hepes, 1% Nonidet P-40, 2 mmol/L Na_3VO_4, 100 mmol/L NaF, 10 mmol/L $PyrPO_4$, 4 mmol/L EDTA, 1 mmol/L phenylmethylsulfonyl fluoride, 1 μg/mL leupeptin, and 1 μg/mL aprotinin). Protein samples were denatured by boiling at 95°C for 5 min, separated on 4–12% Bis-Tris NuPAGE gels (25–40 μg/lane; Invitrogen), and blotted onto a polyvinylidene fluoride membrane (FluoroTrans; Pall Life Sciences, Ann Arbor, MI). Membranes were probed with the following primary antibodies (dilution for all 1:1,000): rabbit anti-CREB/pCREB; rabbit anti-ERK1/2/pERK1/2 (both Cell Signaling); rabbit anti–cyclin A; and rabbit anti–cyclin D1 (both Santa Cruz). After incubation with horseradish peroxidase–conjugated secondary antibody (1:5,000; The Jackson Laboratories), proteins were visualized using enhanced chemiluminescence (Millipore), and levels were quantified using Labworks software (UVP, Upland, CA).

Analytical procedures. Plasma glucose concentrations were measured by the glucose oxidase method (YSI Glucose Analyzer, Yellow Springs, OH). Plasma lipase concentrations were measured by a colorimetric enzyme assay (BioAssay Systems, Hayward, CA).

Statistical analysis. Statistical analysis was performed using the Student t test or ANOVA, where appropriate (Statistica, version 6; Statsoft, Tulsa, OK).

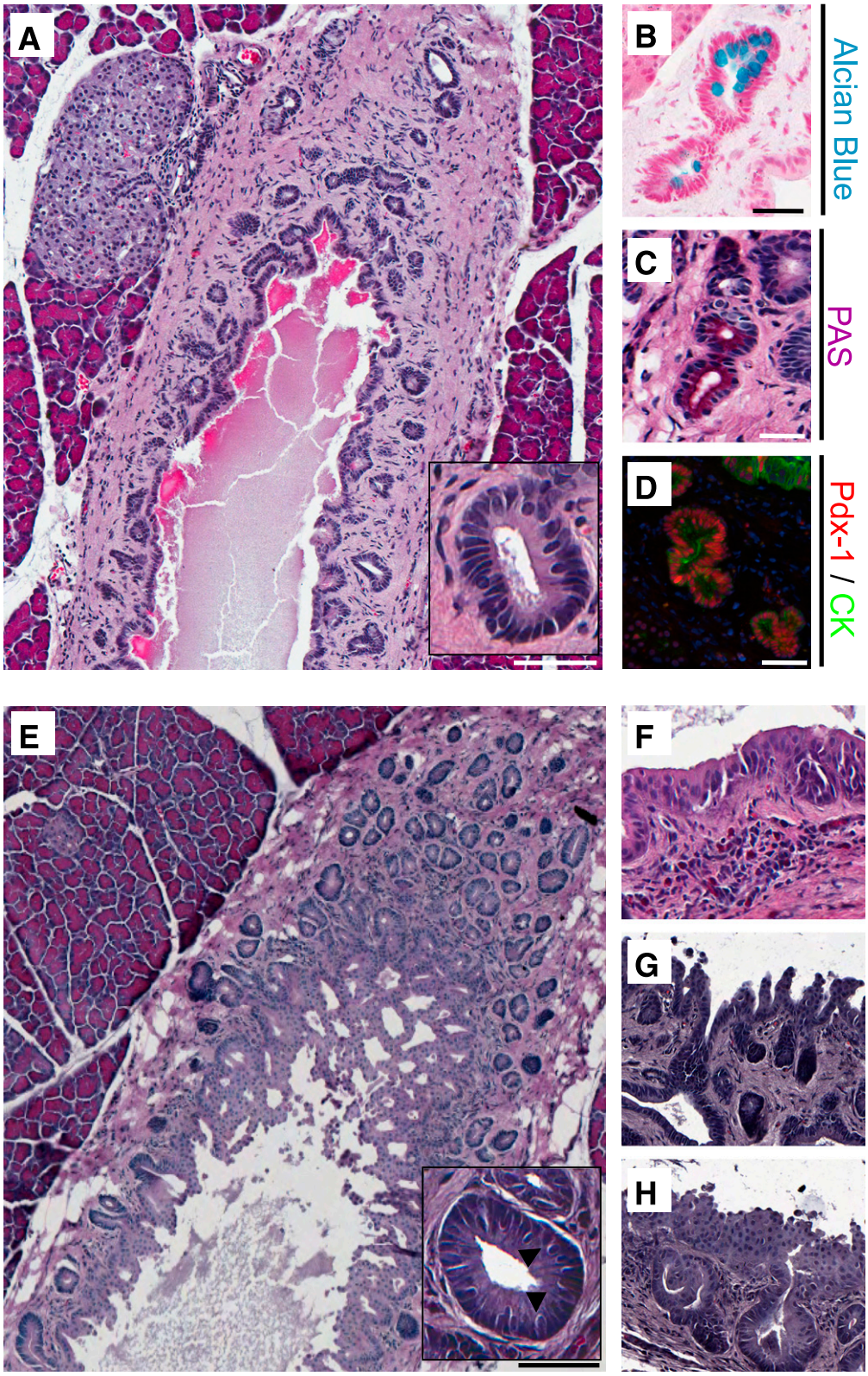

FIG. 1. The extent and frequency of PDGs surrounding the main pancreatic duct are increased by exendin-4 treatment in rats. Sections from the head of the pancreas from an untreated control rat (*A*) and after 12 weeks of daily exendin-4 injections (*E*), in which PDG clusters were identified surrounding the main pancreatic duct. PDGs were confined to the mesenchyme surrounding the main duct in controls but, after exendin-4, expanded to the extent that they projected into the lumen of the pancreatic duct as complex villous-like structures. *A* and *E*, *insets*: PDG cells were columnar in comparison with the cuboidal ductal cells and included goblet-like cells (arrowheads). *B* and *C*: PDGs contained mucin confirmed by Alcian blue and PAS staining. *D*: In contrast to duct cells, PDG cells also expressed Pdx-1 (red; combined staining with the duct cell marker cytokeratin [CK] in green). *E*: PDGs were more common in exendin-4–treated rats (Table 1). *F–H*: In addition, the epithelium often showed pseudostratification and pseudopapillary features, which are features characteristic for PanIN-like lesions. Scale bars = 200 μm (*A* and *E*) and 100 μm (*B–D*), and magnification ×20 (*F–H*). (A high-quality digital representation of this figure is available in the online issue.)

Data in graphs and tables are presented as means ± SEM. Findings were assumed statistically significant at $P < 0.05$.

RESULTS

Metabolic actions of exendin-4 in rats. Twelve weeks of daily exendin-4 injections had the anticipated effects of decreasing weight gain (66 ± 8 vs. 164 ± 5 g; $P < 0.001$ exendin-4 vs. control) and blood glucose levels (99 ± 2 vs. 108 ± 4 mg/dL; $P < 0.01$ exendin-4 vs. control). As expected, exendin-4 decreased daily food intake (153 ± 5 vs. 204 ± 5 mg/day; $P < 0.001$ exendin-4 vs. control), but the treated animals did not seem to be in any apparent pain or distress (Supplementary Fig. 1).

Effects of exendin-4 on exocrine pancreas in rats. Pancreas weight was comparable in the treated versus control group (2.3 ± 0.1 vs. 2.3 ± 0.1 g; exendin-4 vs. control). However, relative to body weight, pancreatic weight in exendin-4–treated animals was increased (0.53 ± 0.02 vs. 0.43 ± 0.02; $P < 0.01$ exendin-4 vs. control) (Supplementary Fig. 1*D*).

There was no histological evidence of pancreatitis in either the exendin-4 or control group. Consistent with this, lipase activity was not changed by exendin-4 (330 ± 19 vs. 299 ± 11 units/L; exendin-4 vs. control) (Supplementary Fig. 1*E*). However, exendin-4 did induce a marked expansion of the PDG compartment (Fig. 1 and Supplementary Fig. 2). PDGs were identified, as previously described, as blind outpouchings from large pancreatic ducts present in the mesenchyme surrounding the ducts. PDG cells were further distinguished from main duct cells by frequently being columnar rather than cuboidal (Fig. 1*A* and *E*, *insets*) and mucin positive (Alcian blue and PAS stains). PDGs also expressed Pdx-1 (Figs. 1*B–D*). There was an ~70% increase in the number of PDGs per unit of length of the main pancreatic duct following exendin-4 treatment (52 ± 7 vs. 31 ± 4 PDGs/mm main duct; $P < 0.05$ exendin-4 vs. control) (Table 1). Moreover, the mean cross-sectional area of individual PDGs still confined within the mesenchyme around the ducts was ~30% increased by exendin-4 treatment (1,184 ± 102 vs. 910 ± 45 μm^2; $P < 0.05$ exendin-4 vs. control), a conservative estimate given that the expanded PDGs adopt a more coiled structure as previously described (19). The latter evaluation also likely underestimates the extent of the expansion of PDGs in exendin-4–treated rats because in many cases the PDGs also expanded into the duct lumen with a complex cribriforming and papillary architecture. To account for this, we quantified the extent to which the main duct lumen was convoluted by any intraluminal projection by computing the ratio of the circumference of the inner duct lumen to the duct length, a metric that was ~35% increased in exendin-4–treated animals (5.0 ± 0.2 vs. 3.7 ± 0.3; $P < 0.01$ exendin-4 vs. control). With exendin-4, the epithelium also showed variable nuclear pseudostratification and loss of polarity, as well as micropapillary architecture (Fig. 1*F–H*), histologic features that can be associated with PanIN lesions and dysplasia when observed in human pancreas, although the implications in rat pancreas are unknown. No carcinoma was seen. Collectively, these findings confirm an increased number of PDGs and expansion of the epithelial cell compartment of both PDGs and large ducts in response to exendin-4 treatment.

The frequency of PDG cell replication was fourfold increased in exendin-4 versus control rats (14.6 ± 3.9 vs. 3.8 ± 0.9%; $P < 0.05$ exendin-4 vs. control) (Fig. 2). The frequency of replication in the main pancreatic ducts was much lower than that in the PDGs but still increased twofold by exendin-4 treatment (5.3 ± 1.8 vs. 2.7 ± 0.6%; $P < 0.05$ exendin-4 vs. control). In contrast, there was no statistically increased frequency of duct cell replication with exendin-4 treatment in the small ducts of the tail of the pancreas (0.62 ± 0.17 vs. 0.42 ± 13%; $P = 0.4$ exendin-4 vs. control).

TABLE 1
Analysis of the PDG compartment

	Control	Exendin-4
Number of PDGs/mm main duct	31 ± 4	52 ± 7*
PDG area (μm^2)	910 ± 45	1,184 ± 102*
Main duct lining-to-length ratio	3.7 ± 0.3	5.0 ± 0.2†

To evaluate the extent of the PDG compartment in treated and control animals, we analyzed the PDG compartment in sections from the head of the pancreas from 10 animals in each group (illustrated in Supplementary Fig. 2). The number of PDGs per millimeter of main duct (first row) and the average size of a PDG (second row) revealed a marked expansion of the PDG compartment after exendin-4 treatment. Furthermore, the main duct appears to be dilated because the ratio of main duct lining to length was increased in the treated group (third row). *$P < 0.05$. †$P < 0.001$.

Actions of GLP-1 mimetic treatment on the exocrine pancreas in the Pdx1-Kras mutant mouse. In Pdx1-Kras mice, 12 weeks of exendin-4 treatment had no impact on body weight (23.2 ± 1.2 vs. 25.8 ± 1.7 g), food intake (18.1 ± 0.7 vs. 19.7 ± 0.5 g per week), or blood glucose levels (83.0 ± 3.4 vs. 75.4 ± 3.7 mg/dL) when compared with littermate control mice. However, GLP-1 mimetic treatment increased pancreatic weight (1.1 ± 0.1 vs. 0.7 ± 0.1 g; exendin-4 vs. control) (Supplementary Fig. 3).

While overall lobular architecture was preserved in both animal groups, the exendin-4–treated animals demonstrated more extensive chronic pancreatitis with greater loss of acini with replacement by reactive or metaplastic duct profiles (Fig. 3). The percentage of pancreas composed of acinar tissue was decreased by 61% by exendin-4 treatment (13.0 ± 13.5% vs. 33.6 ± 14.6%; $P < 0.05$ exendin-4 vs. control). These changes were accompanied by increased inflammation, more extensive stromal fibrosis, and widespread reactive and metaplastic changes, as determined by pancreatitis score (10.0 ± 1.2 vs. 8.6 ± 0.8; $P < 0.05$ exendin-4 vs. control). The plasma lipase activity also was increased with exendin-4 (1,020 ± 164 vs. 678 ± 34 units/L; $P < 0.05$ exendin-4 vs. control) (Supplementary Fig. 3). In comparison to control animals, treated animals showed more extensive acinar-to-ductal metaplasia with replacement of acini by ductules lined by mucin-producing cells primarily with small, round basally oriented nuclei without papillary features (mPanIN1). A minority of the duct profiles demonstrated increased nuclear hyperchromasia and pleomorphism with stratification and micropapillary changes (mPanIN2 and mPanIN3) (Fig. 3). Moreover, GLP-1 mimetic treatment induced increased duct cell proliferation ($P < 0.05$) in Pdx1-Kras mice when compared with control animals (Fig. 4).

GLP-1R expression in PDGs and PanIN lesions. GLP-1R expression was readily detected in pancreatic β-cells in rat and human pancreas, serving as a positive control (data not shown). GLP-1R expression also was present in PDG cells in both rodent and in human pancreas (Fig. 5). GLP-1R expression was not detected in pancreatic acinar cells. GLP-1R expression also was abundantly present in mPanIN lesions

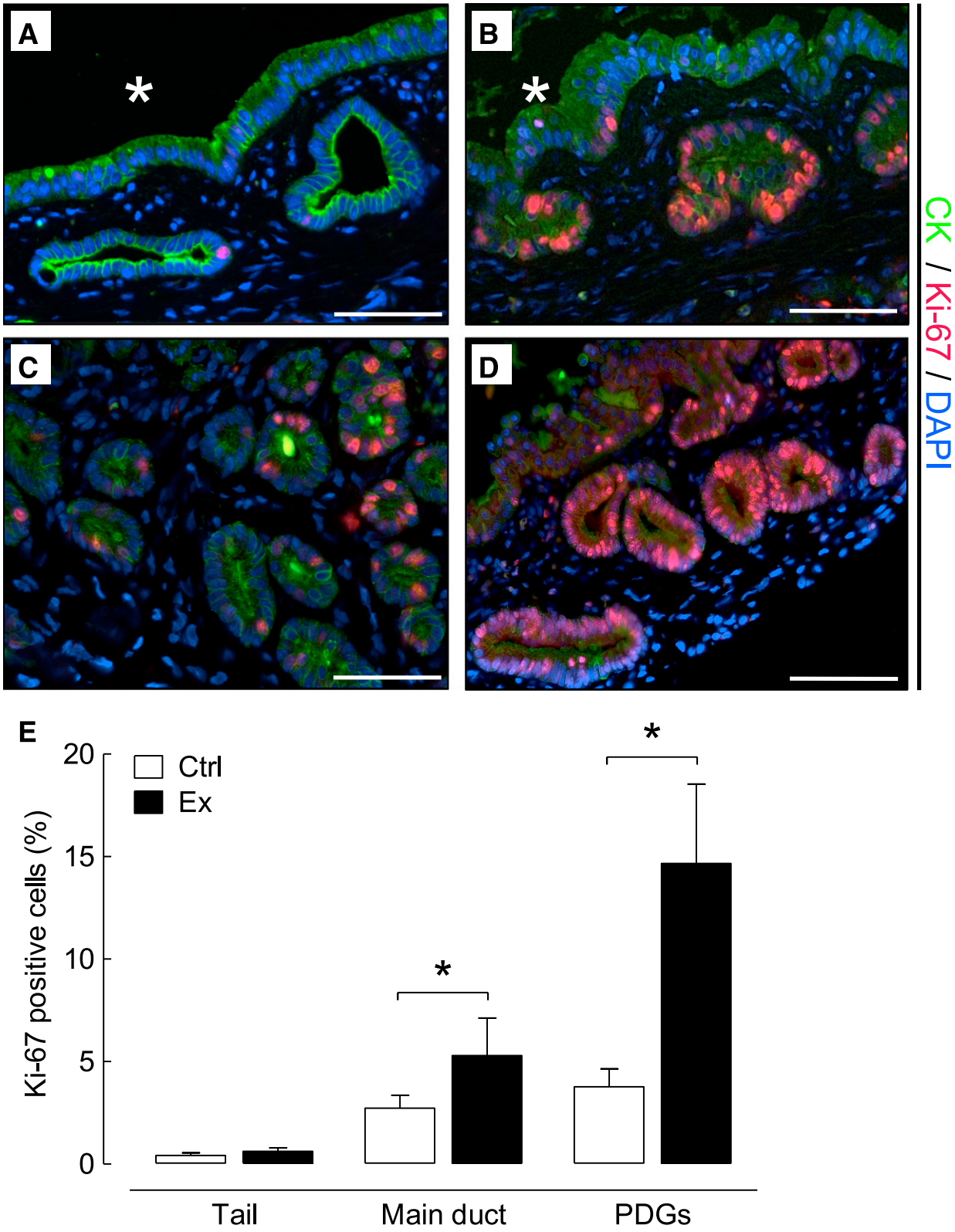

FIG. 2. PDG cell replication is increased by exendin-4 treatment in rats. The frequency of replication ascertained by Ki-67 immunostaining (red; colabeled with cytokeratin [CK] in green) was increased in PDGs compared with adjacent duct cells (*lumen of the large duct) in both control (*A*) and exendin-4–treated (*B*) rats. Replication frequency showed variation within the PDGs in control (*C*) as well as exendin-4–treated (*D*) animals. *E*: However, both the abundance of PDGs and the frequency of replication were increased by exendin-4 treatment. Exendin-4 also increased replication in main duct cells but not in the duct cells in the tail of the pancreas. □, control (Ctrl); ■, exendin-4 (Ex). *$P < 0.05$, scale bars = 100 μm. (A high-quality digital representation of this figure is available in the online issue.)

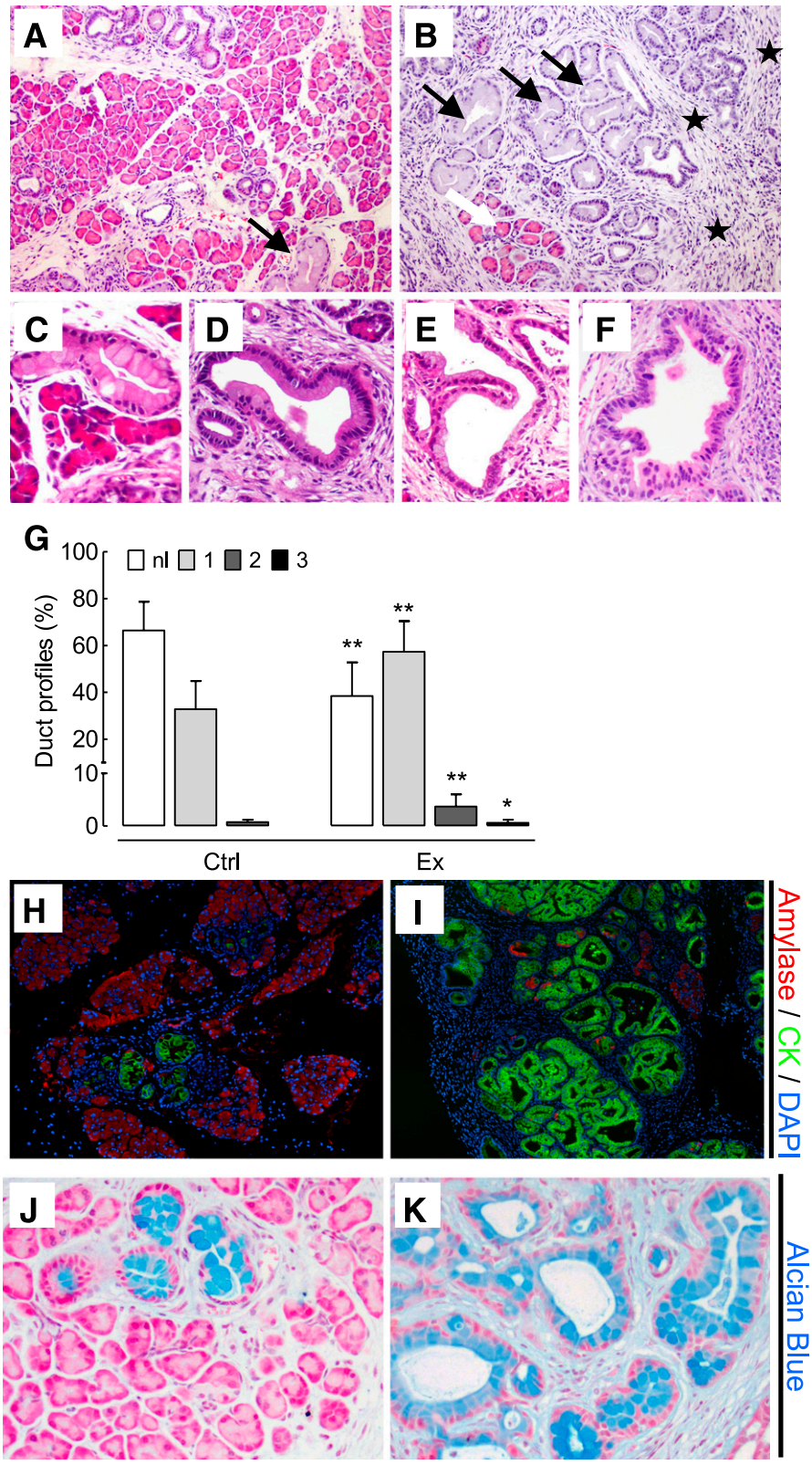

FIG. 3. Exendin-4 treatment increased chronic pancreatitis and the frequency of mPanIN lesions in Pdx1-Kras mice. Pancreata from Pdx1-Kras mice treated for 12 weeks with either vehicle (*A*) or exendin-4 (*B*) (20× objective). The pancreas from the exendin-4–treated animal demonstrates only scant residual intact acini (white arrow) with more extensive inflammation and fibrosis (stars) and more frequent mPanIN (black arrows). *C* and *D*: Low-grade mPanIN1a and mPanIN1b lesions with abundant apical mucin and basally oriented nuclei without significant nuclear pleomorphism or mitotic activity. *E* and *F*: Higher-grade mPanIN2 and mPanIN3 lesions with increased nuclear pleomorphism and focal loss of polarity. *G*: Quantitative analysis of mPanINs showing the percentage of pancreatic ducts with no dysplasia (□, normal [nl]); light-grey box, mPanIN1 (1); medium-grey box, mPanIN2 (2); or ■, mPanIN3 (3) lesions in control (Ctrl) and exendin-4 (Ex)-treated mice. *H*: Combined amylase (red) and cytokeratin (CK; green) immunofluorescent staining of the pancreas of a control Pdx1-Kras mouse. *I*: Intact acinar tissue (red) is replaced by cytokeratin-positive (green) ducts, and amylase-positive cells are rarely found in exendin-4–treated animals. Alcian blue staining (blue; counterstained with Nuclear Fast red) reveals mucin-containing lesions in control mice (*J*) and a higher frequency in treated mice (*K*). *$P < 0.05$; **$P < 0.01$ vs. control. (A high-quality digital representation of this figure is available in the online issue.)

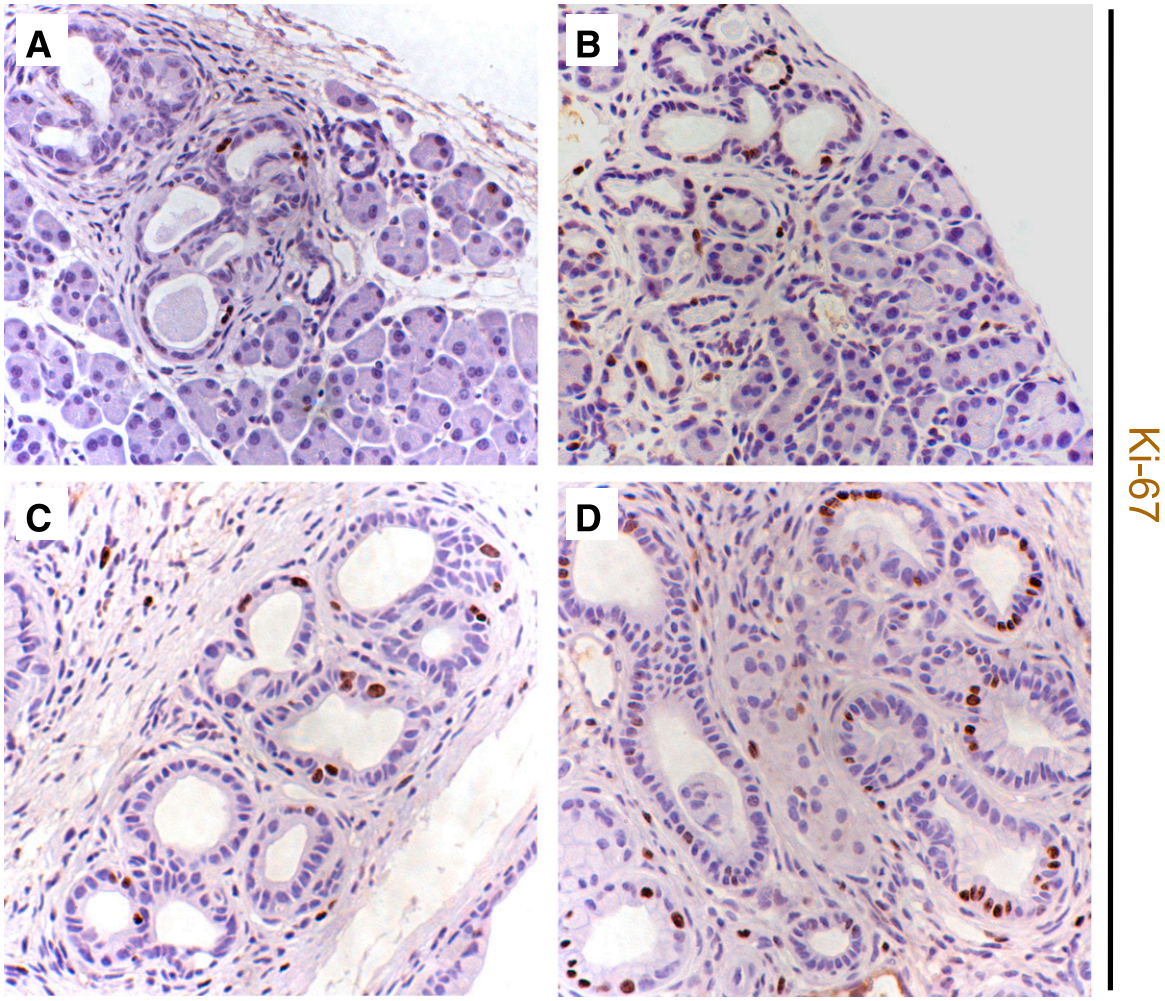

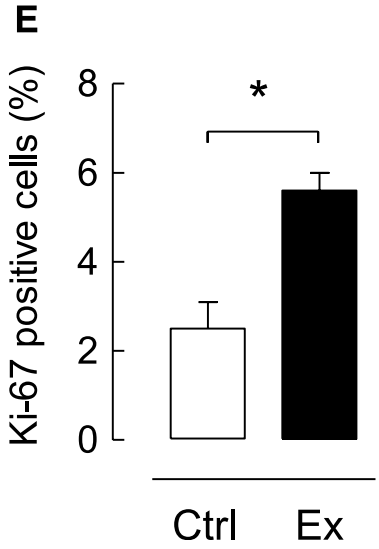

FIG. 4. Duct cell replication frequency is increased in the pancreas of exendin-4–treated Pdx1-Kras mice. Immunohistochemical labeling of Ki-67–positive cells (brown; counterstained with hematoxylin) in benign ducts in areas of intact acinar tissue in control mice (*A*) and exendin-4–treated mice (*B*). An area of ductal proliferation embedded in fibrotic tissue shows an increase in Ki-67–positive cells in the exendin-4–treated group (*D*) compared with controls (*C*). Note the presence of proliferative ducts and mPanIN1a lesion in the exendin-4–treated animal. *E*: Analysis of duct cell proliferation by Ki-67 reveals an increase in the replication frequency in Pdx1-Kras mice treated with exendin-4 (Ex; ■) compared with vehicle control (Ctrl; □). **P* < 0.05. (A high-quality digital representation of this figure is available in the online issue.)

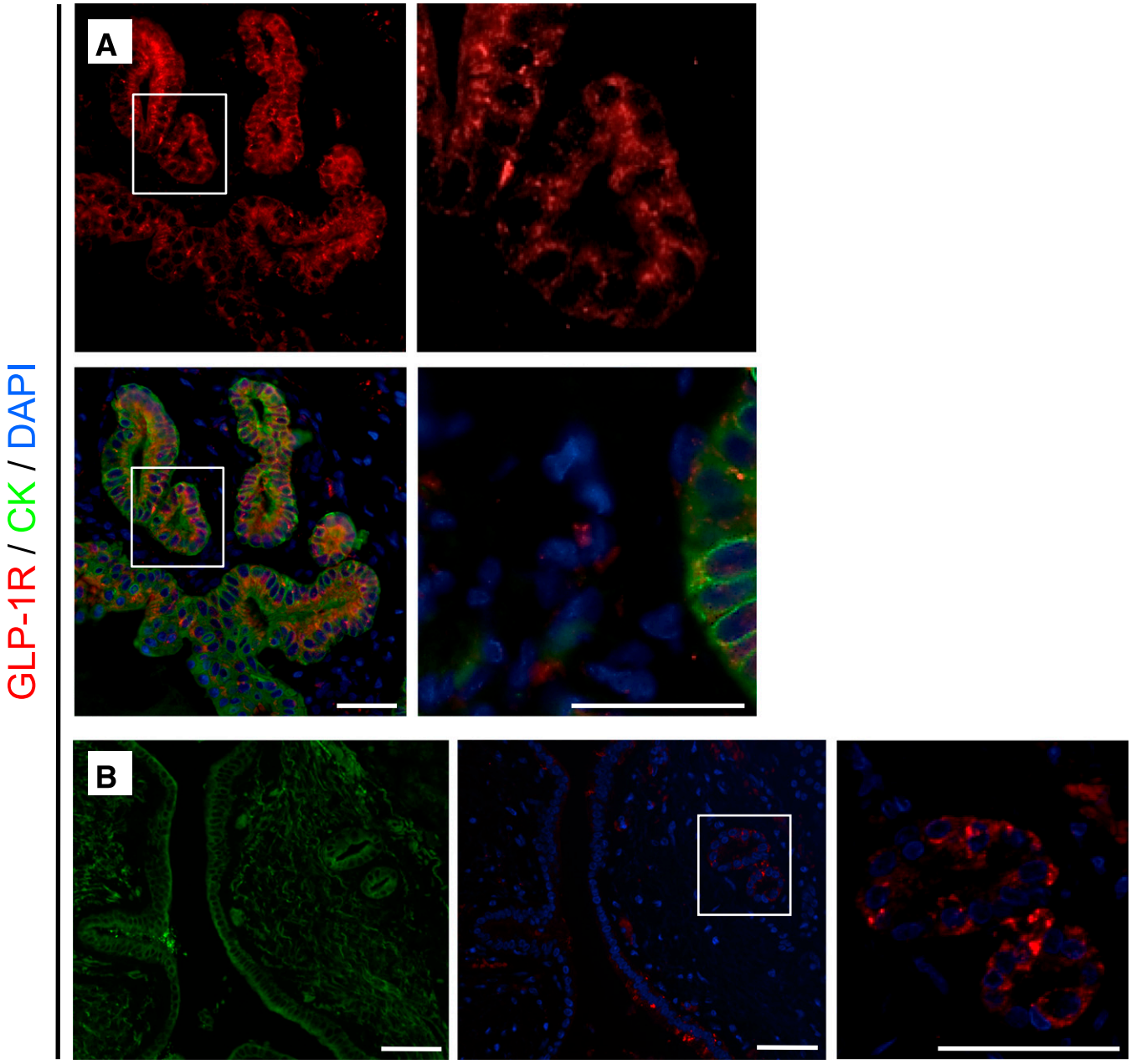

FIG. 5. GLP-1R expression is present in PDGs in rats and humans. *A*: In the PDGs (shown here for an exendin-4–treated rat), GLP-1R expression (red) was detected by immunofluorescence with combined labeling for the duct cell marker cytokeratin (CK) in green and DAPI to mark the nuclei in blue. *B*: Colocalization of GLP-1R and cytokeratin is indicated in the merged images by the color orange. GLP-1R expression was similarly apparent in PDGs in duct cells in the human pancreas. Scale bars = 100 μm. (A high-quality digital representation of this figure is available in the online issue.)

in the pancreas of Pdx1-Kras mice and humans (Fig. 6). GLP-1R was also detected in areas of acinar-to-ductal metaplasia as well as mPanIN lesions in Pdx1-Kras mice (Fig. 6*A* and *B*). In humans, cells with a columnar phenotype had prominent GLP-1R expression. For example, immunoreactivity was present in PanIN1 lesions but only was minimally detected in adjacent cells with normal cuboidal pancreatic duct morphology in the same duct (Fig. 6*C*). In 6 of 10 human pancreata, GLP-1R expression was detected in a variety of ductal lesions (PanIN1a to PanIN3) (Fig. 6*D* and *E*).

Actions of exendin-4 treatment in human pancreatic duct cells. GLP-1 activation of G-protein–coupled receptors has been reported to activate multiple signaling pathways in pancreatic β-cells, such as the cAMP–protein kinase A and the MAPK pathways leading to phosphorylation of CREB with increased cyclin levels and β-cell replication in pancreatic β-cells (30–32).

To investigate the mechanism of GLP-1–induced duct cell proliferation, we treated HPDE cells with exendin-4 (Fig. 7). CREB phosphorylation increased after 10 min of exendin-4 exposure, reaching a plateau at ~30 min (1.8 ± 0.2-fold vs. control; $P < 0.05$; $n = 3$) (Fig. 7*A*). Exendin-4 induced a time-dependent phosphorylation of the mitogen-activated kinases ERK1 (4.8 ± 0.6-fold) and ERK2 (2.7 ± 0.1-fold, respectively, vs. control at 10 min; $P < 0.01$; $n = 3$) (Fig. 7*B*). Consequently, cyclin D1 protein was induced to a maximum at ~6 h (1.5 ± 0.2-fold vs. control; $P < 0.05$; $n = 3$) (Fig. 7*C*). However, no changes were observed in cyclin

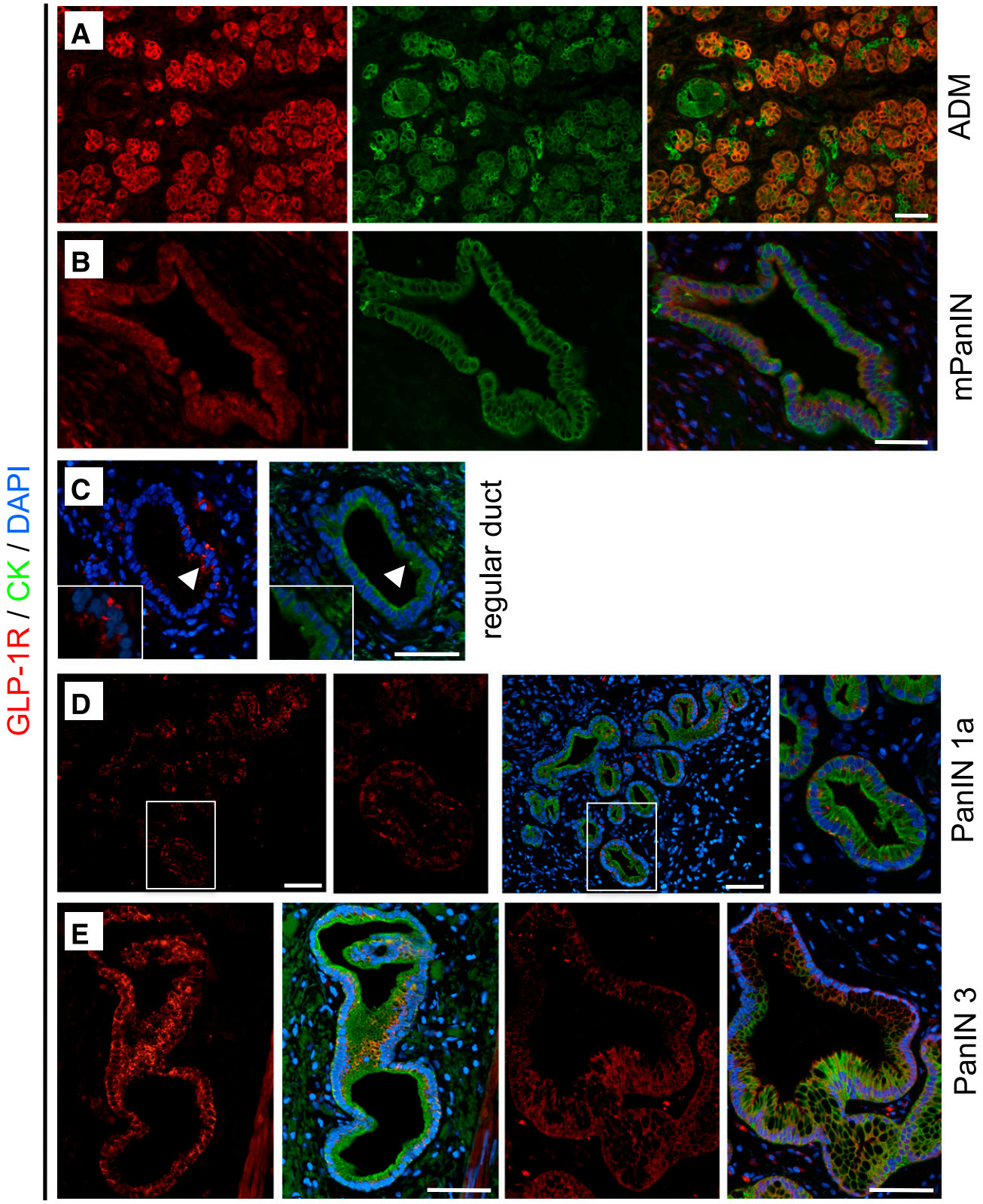

FIG. 6. GLP-1R expression is present in PanIN lesions in Pdx1-Kras mice and humans. GLP-1R (red; shown with combined cytokeratin [CK] labeling in green) was detected in areas of acinar-to-ductal metaplasia (ADM) (*A*) and mPanIN lesion (*B*) in the pancreas of Pdx1-Kras mice. Colocalization of GLP-1R and cytokeratin is indicated in the merged images by the color orange. *C*: In human pancreas, GLP-1R expression was more apparent in the columnar cells (arrowheads) in regular ducts compared with adjacent normal cuboidal duct cells shown away from the arrowhead. *D*: Where duct cells adopt the columnar phenotype (PanIN1a lesion shown), GLP-1R expression becomes more apparent. *E*: In more advanced PanIN3 lesions, GLP-1R immunoreactivity also was clearly present. Scale bars = 100 μm. (A high-quality digital representation of this figure is available in the online issue.)

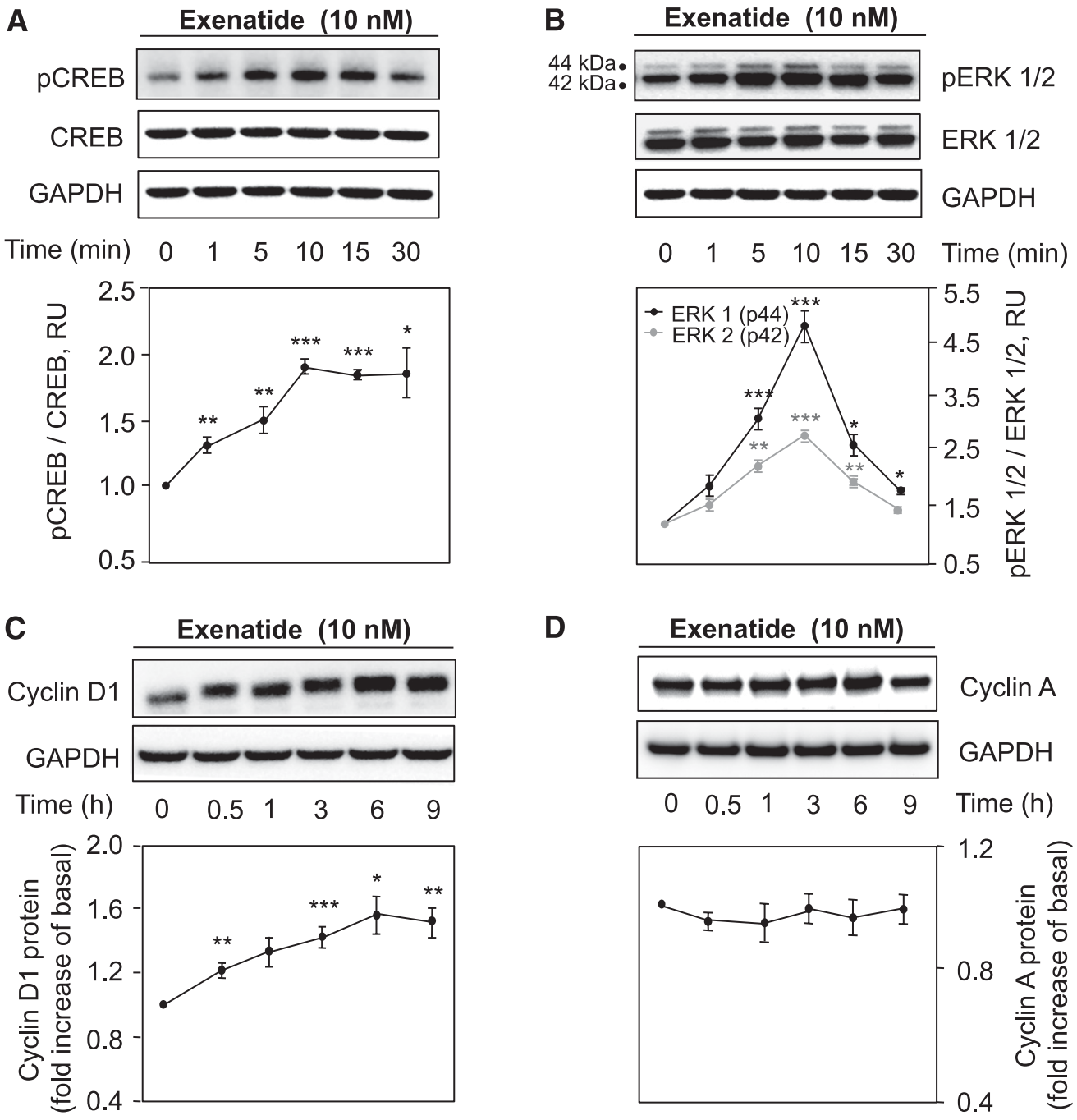

FIG. 7. Exendin-4 actions on human pancreatic duct cells. *A* and *B*: Time-course experiments of CREB (*A*) and ERK1/2 (*B*) phosphorylation in HPDE cells treated with exendin-4 (10 nmol/L) for 0–30 min as indicated. GAPDH, glyceraldehyde-3-phosphate dehydrogenase. Representative examples of Western blot experiments are shown in the *top panels* and the corresponding analysis in the *bottom panels*. *C* and *D*: Effect of long-term (0–9 h) stimulation on cyclin D1 (*C*) and cyclin A (*D*) protein levels. Data are expressed as the mean ± SD density ratio of total CREB, ERK1/2 (*A* and *B*), as well as glyceraldehyde-3-phosphate dehydrogenase (GAPDH) (*C* and *D*) from 3 to 5 independent experiments. *$P < 0.05$; **$P < 0.01$; ***$P < 0.001$ vs. untreated control value.

A levels (Fig. 7*D*). We also investigated the actions of exendin-4 with or without metformin in the presence of the activating Kras mutation in HPDE cells. Exendin-4 induced CREB phosphorylation in control (pBP) cells (1.4 ± 0.1-fold pCREB/CREB vs. control; $P < 0.01$; $n = 3$), an effect that was more pronounced in the presence of mutant Kras (1.7 ± 0.1-fold vs. control; $P < 0.001$; $n = 3$), and this effect was abrogated by metformin pretreatment (1.0 ± 0.1-fold vs. control; $n = 3$; $P < 0.01$ vs. exendin-4 treatment alone) (Fig. 8).

DISCUSSION

The possibility that GLP-1 mimetic therapy might induce sustained proliferative changes in the exocrine pancreas is of concern because therapy for T2DM may be administered for decades (33,34). An increased reported adverse event rate in the U.S. Food and Drug Administration adverse-event reporting system for pancreatitis and pancreatic cancer in patients treated with GLP-1–based therapy underscores this concern (35). Because T2DM with obesity is a risk factor for pancreatitis and pancreatic

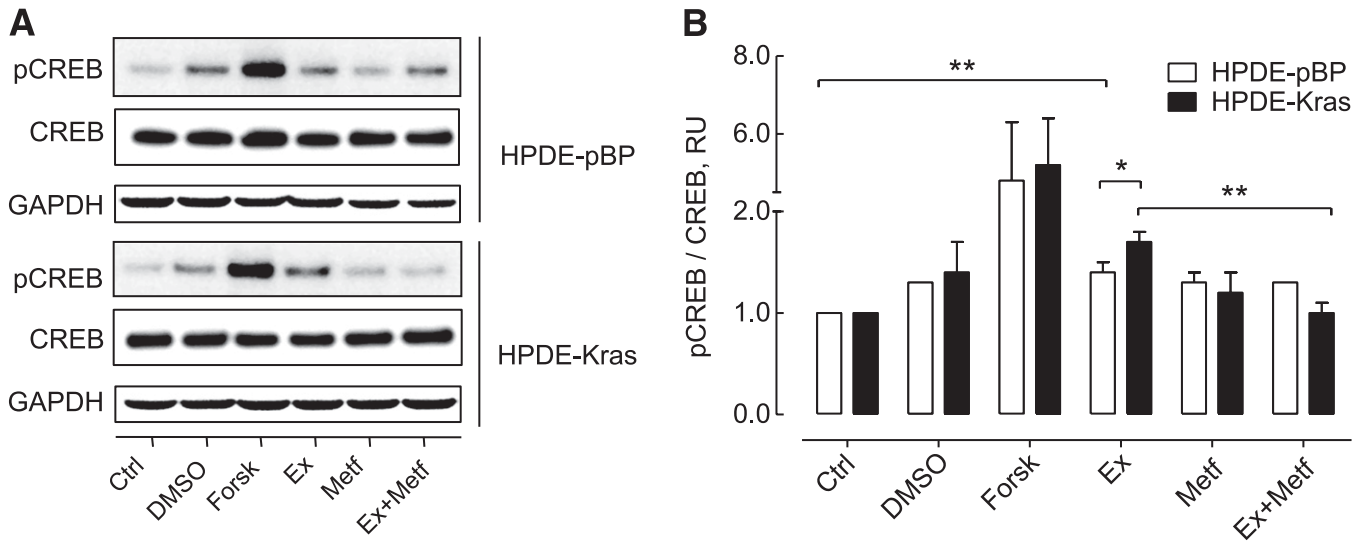

FIG. 8. Oncogenic Kras increases the effects of exendin-4 on human pancreatic duct cells, an effect that is counteracted by metformin. *A*: Representative Western blot of extracts from HPDE cells stably transfected with control vector (pBP) or oncogenic Kras showing CREB phosphorylation at Ser133. Cells were pretreated with metformin (Metf; 100 μmol/L) for 30 min as indicated, prior to a 15-min stimulation with exendin-4 (Ex; 10 nmol/L). Forskolin (Forsk; 10 μmol/L) was used as the positive control. *B*: Statistical analysis shows that phosphorylation of CREB by exendin-4 is higher in HPDE-Kras when compared with HPDE-pBP cells ($P < 0.05$). Metformin treatment abrogated the effect of exendin-4 in HPDE-Kras cells ($P < 0.01$) but not in HPDE-pBP cells. Data are expressed as the mean ± SD density ratio of total CREB from five independent experiments. *$P < 0.05$; **$P < 0.01$. Ctrl, control; DMSO, dimethyl sulfoxide; GAPDH, glyceraldehyde-3-phosphate dehydrogenase.

cancer (36,37), administration of a drug that may further amplify those risks requires closer investigation. In contrast, also unexpectedly, the diabetes medication metformin may decrease the risk of pancreatitis and pancreatic cancer (38,39). Given the recent appreciation that PDGs can give rise to PanIN-like lesions in the context of chronic pancreatitis (19), we first sought to establish the effects of GLP-1R activation on this compartment.

Exendin-4 treatment for 12 weeks induced a marked expansion of the PDG compartment in nondiabetic lean Sprague-Dawley rats. If the pancreas had been sectioned exclusively through the body or tail, no striking abnormalities would have been observed, including no increase in the frequency of replication of duct cells. The normal histology in the most accessible portion of the pancreas and the absence of tumors or overt pancreatitis in lean nondiabetic animals treated with exendin-4 may explain normal exocrine pancreas toxicology screens (40) and some animal studies (17,18). Therefore, to observe the GLP-1–induced changes in PDGs reported in rats here, methodical analysis of the entire pancreas, to include longitudinal sections through the main pancreatic duct, is necessary.

Because PDGs have properties of an adult stem cell compartment (19), it is not surprising that short-term activation of the PDGs by GLP-1 therapy coincident with induced pancreatic injury facilitates recovery from that injury, presumably by fostering regeneration and providing increased protective mucin secretion (17,18). The clinically more relevant question concerns the implication of longer-term stimulation of the PDG compartment and its derivatives.

A total of 12 weeks of exendin-4 therapy in young healthy rats generated mucinous metaplasia and cytologic atypia resembling low-grade PanIN-like lesions in the PDG compartment, features reminiscent of the response to induced chronic pancreatitis in mice and spontaneous chronic pancreatitis in humans (19) (Fig. 1 and Supplementary Fig. 2). However, we also report that GLP-1R expression is present in PDGs and PanIN lesions in rodents and humans, raising the question, does GLP-1 mimetic therapy stimulate the growth of PanIN lesions? Low-grade PanIN lesions are present in 16–80% of normal adult pancreata, the frequency increasing with age (41). PanIN lesions in humans are considered neoplasms and potential precursors for invasive pancreatic cancer based on both pathological findings in humans and longitudinal studies in mice in which mutant Kras is introduced into the pancreas (42). The activating point mutation in the *KRAS* gene is the most frequent mutation present in human PanIN lesions and is considered to be the first step in the progression toward pancreatic cancer (42).

To better appreciate the actions of GLP-1–based therapy in a progression model of PanIN to pancreatic cancer, we treated Pdx1-Kras mice for 12 weeks with exendin-4. Exendin-4 treatment increased duct cell replication, increased the formation of dysplastic mPanIN lesions, and accelerated the development of chronic pancreatitis. These data are consistent with the hypothesis that PanIN lesions contribute to the development of pancreatitis by the obstruction of ductal outflow, with the resulting chronic pancreatitis fostering further development of PanINs (42). The dose of exendin-4 used here, although comparable with that used previously to show the benefit in rodents, exceeds the dose (per kilogram) used in humans (20). A lower dose was used in a recent study to evaluate the effects of exendin-4 on the rodent exocrine pancreas in which no adverse actions were reported (18). However, no data were provided in that report as to whether the dosage of exendin-4 achieved the clinically desired metabolic actions of exendin-4. Moreover, the PDG compartment apparently was not evaluated in those studies, and the animals were not predisposed to dysplasia. It is unknown to date whether a dose of GLP-1 mimetic therapy might be identified that has the intended beneficial actions of enhanced glucose-mediated insulin secretion but no proproliferative effects on the exocrine pancreas.

Evaluation of the proliferative actions of GLP-1 in the exocrine pancreas in humans is not technically feasible. Therefore, we examined the actions of exendin-4 on human pancreatic ductal epithelial cells in vitro. These in vitro studies on the actions of GLP-1R activation in pancreatic duct cells revealed a proproliferative action mediated through the activation of MAPK pathways and phosphorylation of CREB, which was even more apparent in the setting of an activating Kras mutation and inhibited by the actions of metformin. This provides a mechanistic basis for the association of metformin treatment with decreased risk for pancreatitis and pancreatic cancer in individuals with T2DM (38,39). It is also consistent with a previous rodent study in which metformin attenuated the proliferative actions of the DPP-4 inhibitor sitagliptin on the pancreatic ductal tree (3).

In conclusion, we report that treatment of rats for 12 weeks with exendin-4 induced a marked expansion of PDGs through the mechanism of enhanced PDG cell replication. Moreover, we report that the PDGs in rats and humans express GLP-1Rs and that these also are abundantly expressed in PanIN lesions in human pancreas. GLP-1 treatment advances the rate of formation of dysplastic mPanIN lesions and chronic pancreatitis in a mouse model prone to the development of pancreatic ductal adenocarcinoma. Finally, we report that treatment of human pancreatic duct cells with the GLP-1 analog exendin-4 induces proproliferative signaling pathways, an effect that is inhibited by metformin. Collectively, these studies imply that GLP-1–induced proliferation within the exocrine pancreas is focal and may accelerate the development of dysplastic lesions when present.

ACKNOWLEDGMENTS

This work was supported by the National Institute of Diabetes and Digestive and Kidney Diseases, National Institutes of Health, Grant DK-077967 and the Larry Hillblom Foundation.

No potential conflicts of interest relevant to this article were reported.

B.G. performed the studies and assisted in the study design and interpretation and the writing of the manuscript. A.V.M. assisted in executing the study and study interpretation. D.K. assisted in performing the studies and study interpretation. D.D. and S.M.D. assisted in evaluating the histology, interpreting the study findings, and preparing the manuscript. P.C.B. contributed to the study design, study interpretation, and preparation of the manuscript, and is the guarantor of this work and, as such, had full access to all the data in the study and takes responsibility for the integrity of the data and the accuracy of the data analysis.

The authors appreciate the technical assistance of Bonnie Yeh and Rosibel Hernandez and the editorial assistance of Bonnie Lui, from the Hillblom Islet Research Center at UCLA. They also acknowledge the provision of the Pdx1-Kras mouse model by Guido Eibl from the UCLA Center for Excellence in Pancreatic Diseases.

REFERENCES

1. Ebert R, Creutzfeldt W. Gastrointestinal peptides and insulin secretion. Diabetes Metab Rev 1987;3:1–26
2. Xu G, Kaneto H, Lopez-Avalos MD, Weir GC, Bonner-Weir S. GLP-1/exendin-4 facilitates beta-cell neogenesis in rat and human pancreatic ducts. Diabetes Res Clin Pract 2006;73:107–110
3. Matveyenko AV, Dry S, Cox HI, et al. Beneficial endocrine but adverse exocrine effects of sitagliptin in the human islet amyloid polypeptide transgenic rat model of type 2 diabetes: interactions with metformin. Diabetes 2009;58:1604–1615
4. Holst JJ, Vilsbøll T, Deacon CF. The incretin system and its role in type 2 diabetes mellitus. Mol Cell Endocrinol 2009;297:127–136
5. Deacon CF, Holst JJ. Dipeptidyl peptidase IV inhibition as an approach to the treatment and prevention of type 2 diabetes: a historical perspective. Biochem Biophys Res Commun 2002;294:1–4
6. Aschner P, Kipnes MS, Lunceford JK, Sanchez M, Mickel C, Williams-Herman DE; Sitagliptin Study 021 Group. Effect of the dipeptidyl peptidase-4 inhibitor sitagliptin as monotherapy on glycemic control in patients with type 2 diabetes. Diabetes Care 2006;29:2632–2637
7. Fineman MS, Bicsak TA, Shen LZ, et al. Effect on glycemic control of exenatide (synthetic exendin-4) additive to existing metformin and/or sulfonylurea treatment in patients with type 2 diabetes. Diabetes Care 2003;26:2370–2377
8. Pratley RE, Nauck M, Bailey T, et al.; 1860-LIRA-DPP-4 Study Group. Liraglutide versus sitagliptin for patients with type 2 diabetes who did not have adequate glycaemic control with metformin: a 26-week, randomised, parallel-group, open-label trial. Lancet 2010;375:1447–1456
9. Ahmad SR, Swann, J . Exenatide and rare adverse events. N Engl J Med 2008;358:1970–1971; discussion 1971–1972
10. Ayoub WA, Kumar AA, Naguib HS, Taylor HC. Exenatide-induced acute pancreatitis. Endocr Pract 2010;16:80–83
11. Parks M, Rosebraugh C. Weighing risks and benefits of liraglutide: the FDA's review of a new antidiabetic therapy. N Engl J Med 2010;362:774–777
12. Information for healthcare professionals: exenatide (marketed as Byetta): 8/2008 update. Available from http://www.fda.gov/Drugs/DrugSafety/PostmarketDrugSafetyInformationforPatientsandProviders/ucm124713.htm. Accessed 21 December 2011
13. U.S. Food and Drug Administration, Department of Health and Human Services. Sitagliptin (marketed as Januvia and Janumet): acute pancreatitis. 2009. Available from http://www.fda.gov/Safety/MedWatch/SafetyInformation/SafetyAlertsforHumanMedicalProducts/ucm183800.htm. Accessed 21 December 2011
14. Dore DD, Bloomgren GL, Wenten M, et al. A cohort study of acute pancreatitis in relation to exenatide use. Diabetes Obes Metab 2011;13:559–566
15. Perfetti R, Zhou J, Doyle ME, Egan JM. Glucagon-like peptide-1 induces cell proliferation and pancreatic-duodenum homeobox-1 expression and increases endocrine cell mass in the pancreas of old, glucose-intolerant rats. Endocrinology 2000;141:4600–4605
16. Nachnani JS, Bulchandani DG, Nookala A, et al. Biochemical and histological effects of exendin-4 (exenatide) on the rat pancreas. Diabetologia 2009;53:153–159
17. Koehler JA, Baggio LL, Lamont BJ, Ali S, Drucker DJ. Glucagon-like peptide-1 receptor activation modulates pancreatitis-associated gene expression but does not modify the susceptibility to experimental pancreatitis in mice. Diabetes 2009;58:2148–2161
18. Tatarkiewicz K, Smith PA, Sablan EJ, et al. Exenatide does not evoke pancreatitis and attenuates chemically-induced pancreatitis in normal and diabetic rodents. Am J Physiol Endocrinol Metab 2010;299:E1076–E1086
19. Strobel O, Rosow DE, Rakhlin EY, et al. Pancreatic duct glands are distinct ductal compartments that react to chronic injury and mediate Shh-induced metaplasia. Gastroenterology 2010;138:1166–1177
20. Young AA, Gedulin BR, Bhavsar S, et al. Glucose-lowering and insulin-sensitizing actions of exendin-4: studies in obese diabetic (ob/ob, db/db) mice, diabetic fatty Zucker rats, and diabetic rhesus monkeys (Macaca mulatta). Diabetes 1999;48:1026–1034
21. Hingorani SR, Petricoin EF, Maitra A, et al. Preinvasive and invasive ductal pancreatic cancer and its early detection in the mouse. Cancer Cell 2003;4:437–450
22. Gier B, Butler PC, Lai CK, et al. Glucagon like peptide-1 receptor expression in the human thyroid gland. J Clin Endocrinol Metab. 26 October 2011 [Epub ahead of print]
23. Bai H., Li H., Zhang W, et al. Inhibition of chronic pancreatitis and pancreatic intraepithelial neoplasia (PanIN) by capsaicin in LSL-KrasG12D/Pdx1-Cre mice. Carcinogenesis 2011;32:1689–1696
24. Hruban RH, Adsay NV, Albores-Saavedra J, et al. Pathology of genetically engineered mouse models of pancreatic exocrine cancer: consensus report and recommendations. Cancer Res 2006;66:95–106
25. Fendrich V, Chen NM, Neef M, et al. The angiotensin-I-converting enzyme inhibitor enalapril and aspirin delay progression of pancreatic intraepithelial neoplasia and cancer formation in a genetically engineered mouse model of pancreatic cancer. Gut 2010;59:630–637
26. Furukawa T, Duguid WP, Rosenberg L, Viallet J, Galloway DA, Tsao MS. Long-term culture and immortalization of epithelial cells from normal adult

human pancreatic ducts transfected by the E6E7 gene of human papilloma virus 16. Am J Pathol 1996;148:1763–1770
27. Ouyang H, Mou Lj, Luk C, et al. Immortal human pancreatic duct epithelial cell lines with near normal genotype and phenotype. Am J Pathol 2000;157:1623–1631
28. Qian J, Niu J, Li M, Chiao PJ, Tsao MS. In vitro modeling of human pancreatic duct epithelial cell transformation defines gene expression changes induced by K-ras oncogenic activation in pancreatic carcinogenesis. Cancer Res 2005;65:5045–5053
29. Matsuo Y, Campbell PM, Brekken RA, et al. K-Ras promotes angiogenesis mediated by immortalized human pancreatic epithelial cells through mitogen-activated protein kinase signaling pathways. Mol Cancer Res 2009;7:799–808
30. Jhala US, Canettieri G, Screaton RA, et al. cAMP promotes pancreatic beta-cell survival via CREB-mediated induction of IRS2. Genes Dev 2003;17:1575–1580
31. Arnette D, Gibson TB, Lawrence MC, et al. Regulation of ERK1 and ERK2 by glucose and peptide hormones in pancreatic beta cells. J Biol Chem 2003;278:32517–32525
32. Friedrichsen BN, Neubauer N, Lee YC, et al. Stimulation of pancreatic beta-cell replication by incretins involves transcriptional induction of cyclin D1 via multiple signalling pathways. J Endocrinol 2006;188:481–492
33. Butler PC, Dry S, Elashoff R. GLP-1-based therapy for diabetes: what you do not know can hurt you. Diabetes Care 2010;33:453–455
34. Butler AE, Galasso R, Matveyenko A, Rizza RA, Dry S, Butler PC. Pancreatic duct replication is increased with obesity and type 2 diabetes in humans. Diabetologia 2010;53:21–26
35. Elashoff M, Matveyenko AV, Gier B, Elashoff R, Butler PC. Pancreatitis, pancreatic, and thyroid cancer with glucagon-like peptide-1-based therapies. Gastroenterology 2011;141:150–156
36. Noel RA, Braun DK, Patterson RE, Bloomgren GL. Increased risk of acute pancreatitis and biliary disease observed in patients with type 2 diabetes: a retrospective cohort study. Diabetes Care 2009;32:834–838
37. Gumbs AA. Obesity, pancreatitis, and pancreatic cancer. Obes Surg 2008;18:1183–1187
38. Li D, Yeung SC, Hassan MM, Konopleva M, Abbruzzese JL. Antidiabetic therapies affect risk of pancreatic cancer. Gastroenterology 2009;137:482–488
39. Currie CJ, Poole CD, Gale EA. The influence of glucose-lowering therapies on cancer risk in type 2 diabetes. Diabetologia 2009;52:1766–1777
40. Engel SS, Williams-Herman DE, Golm GT, et al. Sitagliptin: review of preclinical and clinical data regarding incidence of pancreatitis. Int J Clin Pract 2010;64:984–990
41. Sipos B, Frank S, Gress T, Hahn S, Klöppel G. Pancreatic intraepithelial neoplasia revisited and updated. Pancreatology 2009;9:45–54
42. Hruban RH, Maitra A, Goggins M. Update on pancreatic intraepithelial neoplasia. Int J Clin Exp Pathol 2008;1:306–316